



## Influence of baffle position on liquid sloshing during braking and turning of a tank truck

Ning KANG<sup>†</sup>, Kui LIU

(School of Transportation Science and Engineering, University of Aeronautics and Astronautics, Beijing 100191, China)

<sup>†</sup>E-mail: kangning@buaa.edu.cn

Received Aug. 23, 2009; Revision accepted Dec. 12, 2009; Crosschecked Mar. 31, 2010

**Abstract:** The influence of baffle position on liquid sloshing during the braking and turning of a tank truck was studied using a volume of fluid (VOF) model. The forces, their positions and weight distribution during braking and the forces and rolling moment during turning were calculated. The reliability of the calculation method was validated by comparisons with experimental results. The results showed that during braking, liquid splashes in the tank and the maximum forces and  $G$  (the ratio of weight acting on the front axle to the rear axle) are large when  $A$  (the ratio of the arch area above the baffle to the area of cross section)  $\leq 0.1$ . When  $A \geq 0.2$ , as the position of the baffle is lowered, the maximum of  $F_x$  (the force in direction  $x$ ) first decreases then increases, and the maximum of  $F_y$  (the force in direction  $y$ ) and  $G$  increase. During turning, liquid splashes in the tank and the maximum forces and  $M$  (the rolling moment) are large when  $D$  (the ratio of the arch area above the baffle to the area of cross section)  $\leq 0.2$ . When  $D \geq 0.3$ , as the position of the baffle is lowered, the maximums of  $F_y$ ,  $F_z$  (the force in direction  $z$ ) and  $M$  increase.

**Key words:** Tank truck, Volume of fluid (VOF) method, Liquid sloshing, Two phase flow, Baffle

**doi:** 10.1631/jzus.A0900521

**Document code:** A

**CLC number:** U469.6

### 1 Introduction

When a tank truck is moving during braking, turning, or bumping, the liquid in the partially filled tank will slosh or even splash due to the oscillation of the unrestrained free surface of the liquid. An additional impact force will act on the tank which offsets the truck's centre of gravity. In such circumstances, an accident may result from wandering, rolling over or from prolonging the stopping distance when braking. During braking, the unsteady weight distribution due to liquid sloshing will reduce the working life of tires and other parts. The study of liquid sloshing in tank trucks can provide data on the forces acting on the tank which can be used for simulating handling stability.

Many general and basic problems of liquid sloshing have been studied. Most studies involved simple tank structures (Armenio, 1996; Romero *et al.*,

2005), but the inner structures of liquefied petroleum gas tank trucks are complex. There are many large baffles in a tank truck. Sometimes the truck moves with uneven speed and in practice there are also complicated dynamic fluid-structure coupling problems (Armenio, 1996; Kim and Yun, 1997). Most current studies of this kind are in the field of aeronautics and astronautics (Yue *et al.*, 1996). Liao *et al.* (1999) studied the additional stress caused by storing liquid in a vessel during emergency braking. The stress on vessels with different border-length or height-diameter ratios was analysed. Bao (2002) investigated the characteristic problem of liquid sloshing in a Dewar flask. The boundary value problem of the differential equation of liquid sloshing was transformed into the extreme-value problem of a function in integral form. Based on the extreme-value principle, the eigen-frequencies of the Dewar, a spherical and a cylindrical container were obtained. Gedikli and Erguven (2003) investigated the effect of a rigid baffle on the natural frequencies of the liquid

in a cylindrical rigid container using a variational boundary element (VBEM) based on Hamilton's principle. Cho and Lee (2004) introduced a velocity-potential-based nonlinear finite element method for the accurate simulation of large amplitude liquid sloshing in a 2D baffled tank subject to horizontal forced excitation. Chen (2006) studied liquid sloshing and the 3D free surface of the liquid in a transportable pressure vessel using a numerical method. He measured the sloshing liquid forces acting on the rigid wall of the vessel and on a baffle inside the vessel which prevented liquid sloshing. The potential for baffles to increase the hydrodynamic damping of sloshing in circular-cylindrical storage tanks was investigated by Maleki and Ziyaeifar (2008). Both horizontal ring and vertical blade baffles were considered. An estimation of the hydrodynamic damping ratio of liquid sloshing in baffled tanks undergoing horizontal excitation was developed analytically using Laplace's differential equation solution. Hasheminejad and Aghabeigi (2009) used linear potential theory to study the natural sloshing frequencies of transverse modes in a cylinder container with or without a pair of inflexible baffles. Successive conformal coordinate transformations in conjunction with the method of separation of variables and the relevant boundary conditions were used to obtain standard truncated matrix eigen-value problems. Eswaran *et al.* (2009) analyzed sloshing waves for baffled and un-baffled tanks. Numerical simulations were carried out based on volume of fluid (VOF) techniques with arbitrary-Lagrangian-Eulerian (ALE) formulation. This approach adopts the displacement of a solid and the pressure and displacement in the fluid as variables to model the coupled system. 3D liquid sloshing in a tank with baffles was studied using the spatially average Navier-Stokes equations (Liu and Lin, 2009). The large-eddy-simulation approach and the second-order accurate VOF method were employed. Panigrahy *et al.* (2009) carried out a series of experiments using a liquid sloshing setup. He estimated the pressure developed on the tank walls and the free surface displacement of water from the mean static level in relation to the changing excitation frequency of the shaking table and the fill level in the tank with and without baffles.

In this paper, numerical simulation of liquid sloshing during the braking and turning of a tank truck with a baffle set at different positions was

conducted using the computational fluid dynamics (CFD) software fluent. The influence of baffle position on the forces, their positions and weight distribution during braking, and on the forces and rolling moment during turning were studied.

## 2 Computational model and method

### 2.1 Governing equations

In this study, the VOF method was adopted to simulate the two phase flow inside a tank truck. The flow is unsteady turbulent flow produced by the interaction of gas and liquid phases. The governing equations are as follows:

Continuity equation:

$$\frac{\partial \rho}{\partial t} + \frac{\partial \rho u_i}{\partial x_i} = 0. \quad (1)$$

Momentum equation:

$$\frac{\partial \rho u_i}{\partial t} + \frac{\partial}{\partial x_j} (\rho u_i u_j) = -\frac{\partial p}{\partial x_i} + \frac{\partial}{\partial x_j} \left[ \mu \left( \frac{\partial u_i}{\partial x_j} + \frac{\partial u_j}{\partial x_i} \right) \right], \quad (2)$$

where  $u$  and  $p$  are velocity and pressure, respectively. As the VOF method was adopted,  $\rho$  and  $\mu$  are the average density and dynamic viscosity based on the volume fraction, respectively.

$$\rho = \alpha_w \rho_w + (1 - \alpha_w) \rho_a, \quad (3)$$

$$\mu = \alpha_w \mu_w + (1 - \alpha_w) \mu_a, \quad (4)$$

where  $\alpha_w$  is the liquid volume fraction,  $\rho_w$  and  $\rho_a$  are the liquid and gas densities, respectively, and  $\mu_w$  and  $\mu_a$  are the liquid and gas viscosities, respectively. The  $\kappa$ - $\varepsilon$  turbulent model was adopted to simulate the turbulent flow.

### 2.2 Tank model and computational grid

The tank studied in this research was a horizontal cylindrical container of circular cross section used as a liquefied petroleum gas tank truck. The total length of the tank was 8.6 m and the inner diameter was

2.254 m. The inner space was divided by baffles into four compartments of roughly equal size. The thickness of the baffle between each compartment was neglected. The length of each compartment was 2.15 m (Fig. 1). The front axle was located at the center of the front wheel and the rear axle was located at the center between the two back wheels.

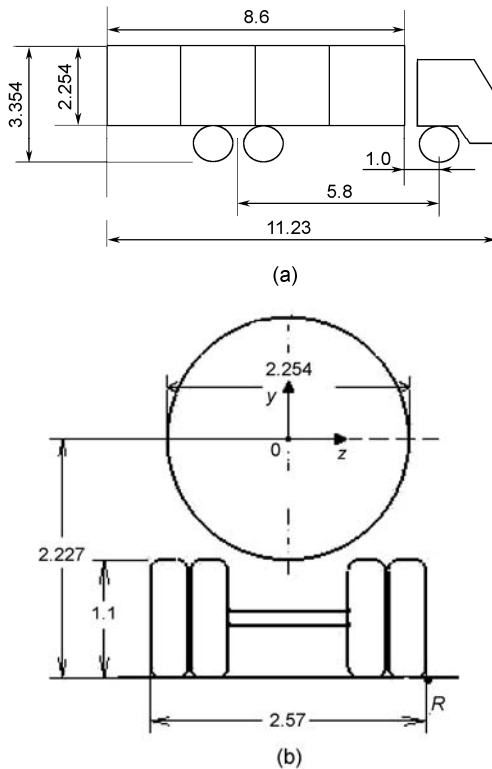


Fig. 1 Profiles of tank truck. (a) Side view and (b) back view of tank truck (unit: m)

Since liquid sloshing in each of the four compartments is the same during braking and nearly the same during turning, the forces acting on each compartment are the same during braking and nearly the same during turning. To reduce the number of grids and the time cost of computation, only one compartment is considered. There is one baffle in a compartment. The origin is located at the center of the left end face of the compartment (Fig. 2). Axis  $x$  is pointing in the direction of the front of the truck.

Since the thickness of the baffle is far less than the size of the compartment, the thickness of the baffle is neglected. The computational domain is the inside volume of one compartment and is divided into structured hexahedral elements. The total number of elements is  $4 \times 10^4$  (Fig. 2).

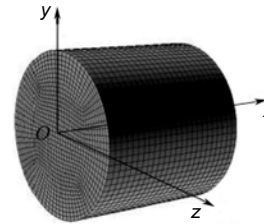


Fig. 2 Mesh of computational domain

### 2.3 Boundary and initial conditions

The boundary condition of the inside surfaces of one compartment and the surfaces of the baffle are no slip wall boundary condition. At initial moment, the interface between the gas and liquid phases is parallel to the  $xz$  plane. The velocities of the gas and liquid phases relative to the compartment are zero. The pressure of the gas phase is  $1.01 \times 10^5$  Pa.

### 2.4 Computational method and parameters

The coupling between pressure and velocity is via the pressure implicit split-operator (PISO) algorithm. The pressure-correction equation is discretized with the body force weighted scheme. The convective term is discretized with the first-order upwind scheme.

The gas and liquid phases are air and oil, respectively. Air is taken to be an ideal compressible gas with a dynamic viscosity of  $1.81 \times 10^{-5}$  kg/(m·s). Oil density is  $830$  kg/m<sup>3</sup> and dynamic viscosity is  $3.32 \times 10^{-3}$  kg/(m·s). The time step of unsteady calculation is 0.005 s.

## 3 Validation of computational method

To verify the accuracy of the computational method used in this study, the calculated sloshing frequencies were compared with the test results of Li *et al.* (2007). Li *et al.* (2007)'s model was also a horizontal cylindrical container of circular cross section, with a length of 0.310 m and a radius of 0.145 m. The media inside the container were air and water.

The container and the media inside moved together along axis  $z$  with a velocity of 0.1 m/s (Fig. 1). At the initial moment  $t=0$ , the container suddenly stopped moving and then sloshing occurred periodically inside the container.

In this study, liquid transverse sloshing frequencies were calculated for seven liquid filling ratios

from 0.2 to 0.8. The calculated frequencies and the test results are listed in Table 1. The errors between them are within 7.27%. Therefore, the computational method used in this study was verified.

**Table 1 Computational and test results**

Filling ratio	Test result (Hz)	Computational result (Hz)	Error (%)
0.2	1.288	1.389	7.27
0.3	1.384	1.423	2.74
0.4	1.401	1.463	4.24
0.5	1.406	1.515	7.19
0.6	1.591	1.562	1.82
0.7	1.688	1.675	0.78
0.8	1.766	1.763	0.17

**4 Computational results and analysis**

**4.1 Liquid sloshing during braking**

The baffle was located on the plane of  $x=1.075$  m (Fig. 3).  $S_2$  is the area of the baffle, and  $S_1$  and  $S_3$  are the arch areas over and under the baffle, respectively. The followings are the definitions of  $A$  and  $B$ :

$$A = \frac{S_1}{S_1 + S_2 + S_3}, \quad B = \frac{S_2}{S_1 + S_2 + S_3}. \quad (5)$$

According to legislation, the baffle in tank:  $A \leq 0.2, B \geq 0.4$ .

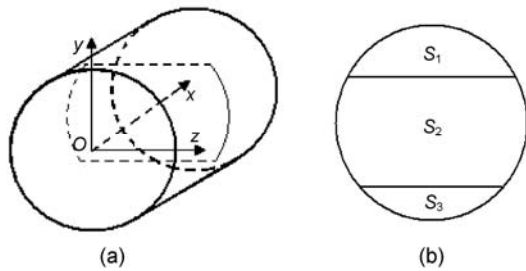


**Fig. 3 Profiles of the baffle during braking. (a) Direction x; (b) Direction y**

The liquid filling ratio was 0.85. The tank truck was moving with a uniform speed before braking. At the moment  $t=0$ , the tank truck started braking with a deceleration  $a=7.5 \text{ m/s}^2$ . In this study, six cases were calculated for  $B=40\%$  and  $A$  from 0.1 to 0.6. The absolute values of forces acting in a single compartment in directions  $x$  and  $y$  at different moments are given in Figs. 4a and 4b.  $F_x$  is in the direction of axis  $x$  and  $F_y$  is in the opposite direction, along axis  $y$ .

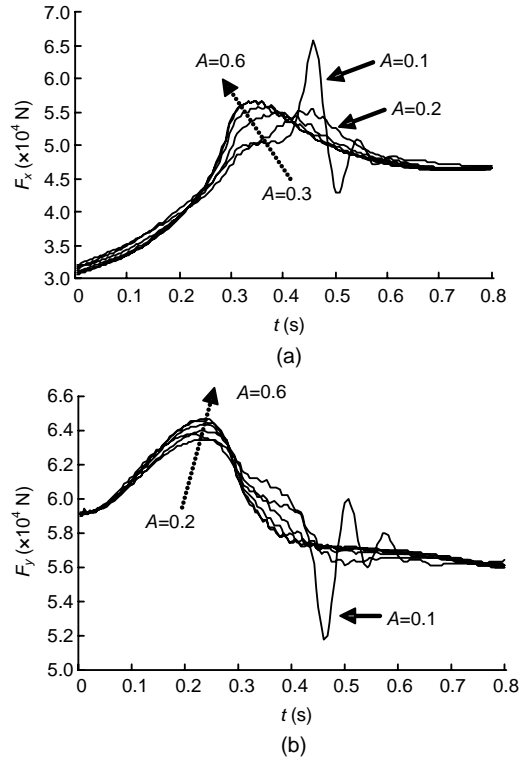


**Fig. 4 Force in directions (a) x and (b) y during braking**

Figs. 4a and 4b show that the curve for  $A=0.1$  is obviously different from the others, having a significant crest and trough around  $t=0.45$  s. The other curves show regular variation.

Figs. 5–7 show liquid sloshing on the cross section of  $z=0$  at different moments for  $A=0.1, A=0.2$  and  $A=0.3$ , respectively. The light shading represents the gas phase and the dark shading represents the liquid phase.

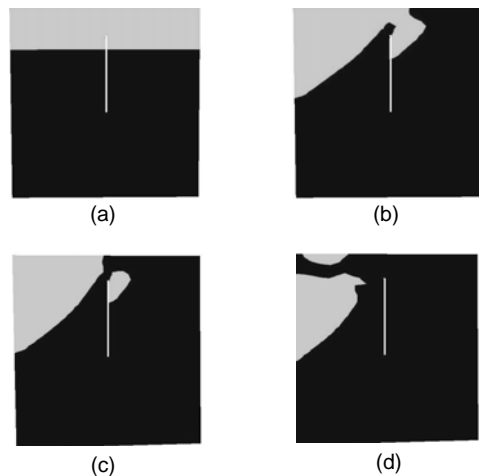


**Fig. 5 Distribution of two phases during braking,  $A=0.1$ . (a)  $t=0.00$  s; (b)  $t=0.40$  s; (c)  $t=0.45$  s; (d)  $t=0.65$  s**

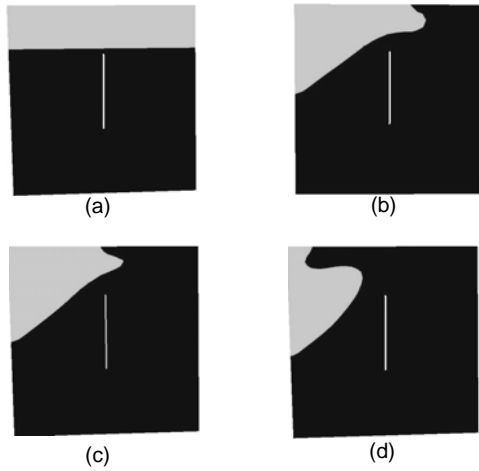


**Fig. 6** Distribution of two phases during braking,  $A=0.2$ . (a)  $t=0.00$  s; (b)  $t=0.40$  s; (c)  $t=0.45$  s; (d)  $t=0.65$  s

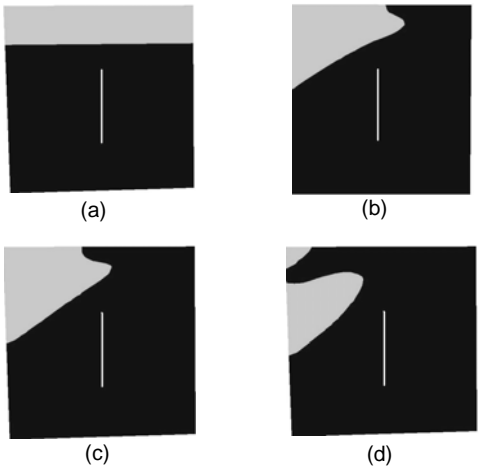


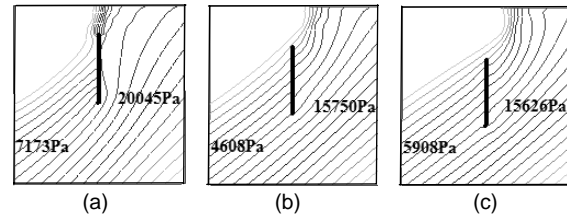
**Fig. 7** Distribution of two phases during braking,  $A=0.3$ . (a)  $t=0.00$  s; (b)  $t=0.40$  s; (c)  $t=0.45$  s; (d)  $t=0.65$  s

Figs. 5–7 show that liquid splashing produced by the baffle at  $A=0.1$  causes the significant crest in Fig. 4a. When the baffle is moved downwards ( $A \geq 0.2$ ), it is totally immersed during the entire braking process. Liquid splashing disappears and the forces vary regularly again.

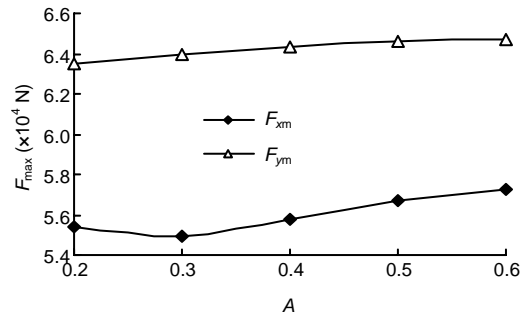
Fig. 8 shows the pressure distribution on the cross section of  $z=0$  at the moment of the appearance of the crests at  $A=0.1$ ,  $A=0.2$  and  $A=0.3$  in Fig. 4a. The pressure is the average pressure acting on each side of the baffle. The differences in pressure on each side in the above three cases are 12 872 Pa, 11 142 Pa and 9718 Pa, respectively. It is apparent that the biggest pressure difference at  $A=0.1$  produces the significant force crest in direction  $x$ .

Fig. 9 shows the maximum forces with the baffle

in different positions. When  $0.2 \leq A \leq 0.6$ , the lower the position of the baffle, the larger is the force in direction  $y$ . The force in direction  $x$  decreases first and then increases, reaching the minimum at  $A=0.3$ . Thus, a baffle can reduce the forces acting on the tank at  $0.2 \leq A \leq 0.3$ .



**Fig. 8** Pressure distributions at crest moments during braking. (a)  $A=0.1$  ( $t=0.45$  s); (b)  $A=0.2$  ( $t=0.45$  s); (c)  $A=0.3$  ( $t=0.40$  s)



**Fig. 9** The maximum of  $F_x$  and  $F_y$  during braking

The positions acted upon by forces  $F_x$  and  $F_y$  with the baffle in different positions are shown in Figs. 10a and 10b.

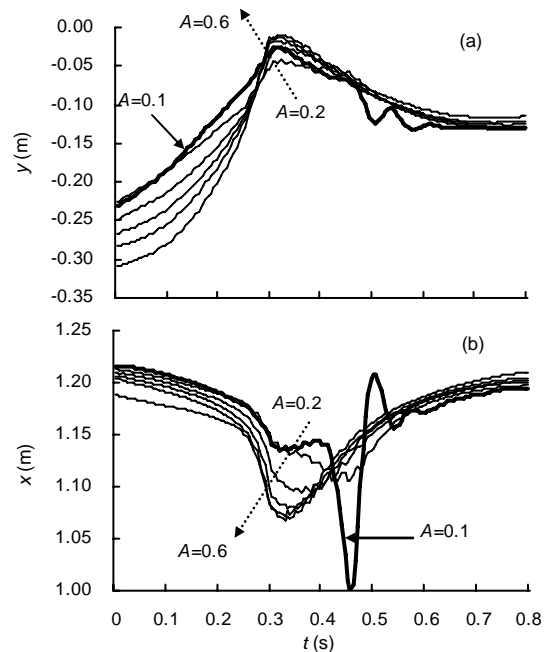


**Fig. 10** Positions of (a)  $F_x$  and (b)  $F_y$  during braking

The highest position of  $F_x$  becomes higher and the position of  $F_y$  moves backwards as the position of the baffle is lowered.

The weight distribution of the entire vehicle is changed as a consequence of braking. The forces of the liquid in the four compartments of the tank truck acting on the front and back axles can be obtained from the results of a single compartment. The weight distribution  $G$  is defined as the ratio of the force on the front axle to the force on the rear axle. Fig. 11 gives the variation in the weight distribution in relation to the position of the baffle. The dotted line represents the weight distribution when the tank truck is moving with a uniform speed.

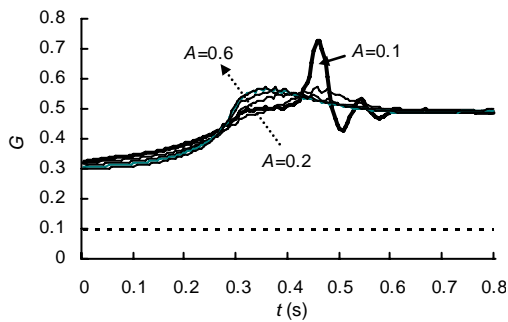


Fig. 11 Weight distribution during braking

The weight distribution during braking is greater than that at a uniform speed. The curve of  $A=0.1$  differs from the others. There is a significant crest around  $t=0.45$  s. When  $0.2 \leq A \leq 0.6$ , the weight distribution increases with the baffle in lower positions.

4.2 Liquid sloshing during turning

The baffle was located on the plane of  $z=0$  (Fig. 12). The area of the baffle is  $S_5$ , and the arch areas over and under the baffle are  $S_4$  and  $S_6$ , respectively. The followings are the definitions of  $C$  and  $D$ :

$$C = \frac{S_5}{S_4 + S_5 + S_6}, \quad D = \frac{S_4}{S_4 + S_5 + S_6}. \quad (6)$$

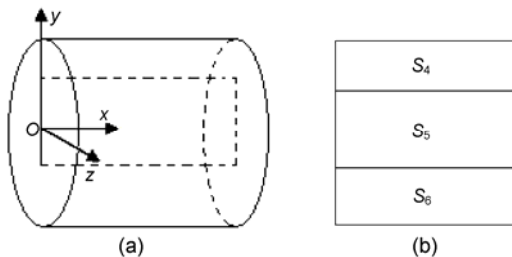


Fig. 12 Profiles of the baffle during turning. (a) Direction  $z$ ; (b) Direction  $y$

The liquid filling ratio was 0.85. The tank truck was moving with a uniform speed before turning. At the moment  $t=0$ , the tank truck started turning with a centripetal acceleration  $a=8$  m/s<sup>2</sup>. Six cases were calculated for  $C=40\%$ , and  $D$  from 0.1 to 0.6. The absolute values of  $F_y$  and  $F_z$  at different times are given in Figs. 13a and 13b.  $F_y$  is in the opposite direction of axis  $y$ , and  $F_z$  is in the direction of axis  $z$ .

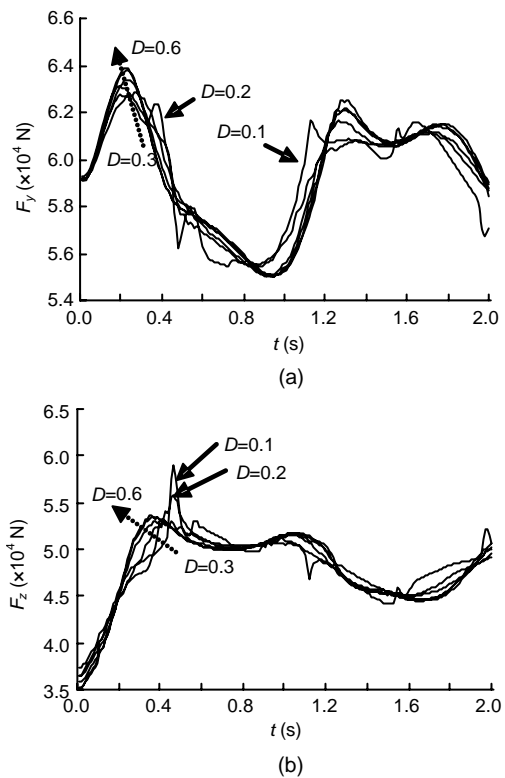
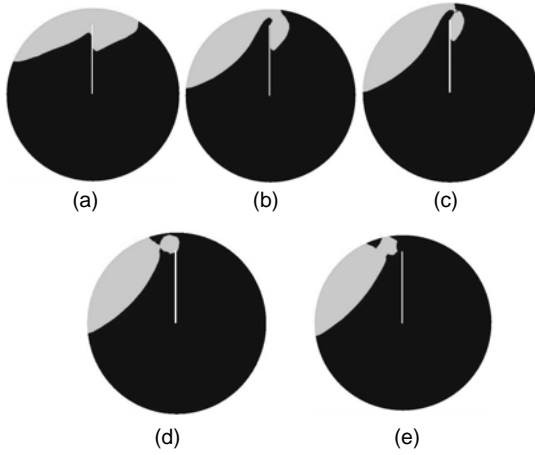


Fig. 13 Force in direction (a)  $y$  and (b)  $z$  during turning

The curves of  $D=0.1$  and  $D=0.2$  are obviously different from the others. There are two significant crests around  $t=0.5$  s for  $D=0.1$  and  $D=0.2$  (Fig. 13b). The other curves show regular variation.

Figs. 14–16 show liquid sloshing on the cross section of  $x=1.075$  at different moments for  $D=0.1$ ,  $D=0.2$  and  $D=0.3$ , respectively.

The cause of the significant crest is the same as mentioned above. Fig. 17 shows the pressure distribution on the cross section of  $z=0$  at the moment of the crests at  $D=0.1$ ,  $D=0.2$  and  $D=0.3$  in Fig. 13b. The differences in pressure on each side of the baffle for the above three cases are 11 183 Pa, 10 063 Pa and 8508 Pa, respectively. It appears that the greater pressure differences at  $D=0.1$  and  $D=0.2$  produce the significant force crests in direction  $z$ .



**Fig. 14** Distribution of the two phases during turning,  $D=0.1$ . (a)  $t=0.20$  s; (b)  $t=0.40$  s; (c)  $t=0.45$  s; (d)  $t=0.55$  s; (e)  $t=0.60$  s

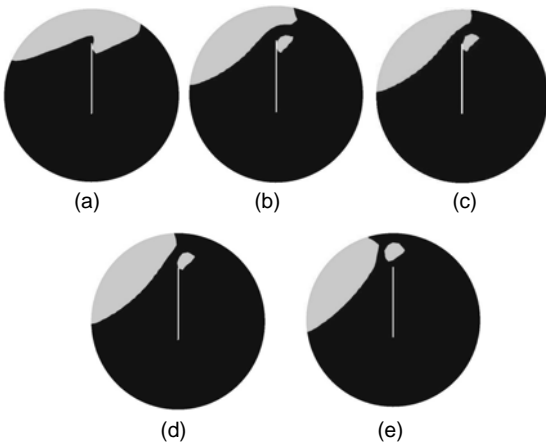


**Fig.15** Distribution of the two phases during turning,  $D=0.2$ . (a)  $t=0.20$  s; (b)  $t=0.40$  s; (c)  $t=0.45$  s; (d)  $t=0.55$  s; (e)  $t=0.60$  s

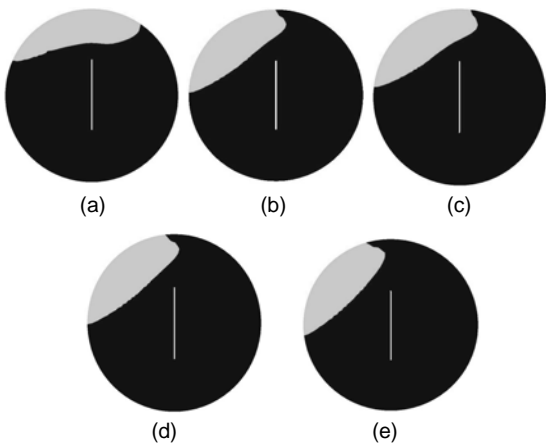


**Fig. 16** Distribution of the two phases during turning,  $D=0.3$ . (a)  $t=0.20$  s; (b)  $t=0.40$  s; (c)  $t=0.45$  s; (d)  $t=0.55$  s; (e)  $t=0.60$  s

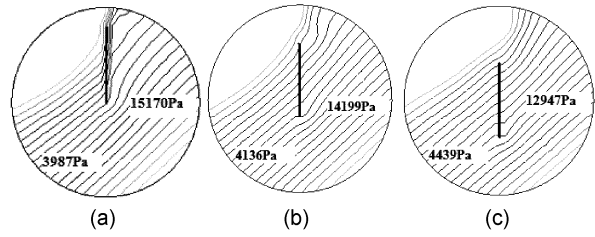


**Fig. 17** Pressure distributions at crest moments during turning. (a)  $D=0.1$ , ( $t=0.46$  s); (b)  $D=0.2$  ( $t=0.46$  s); (c)  $D=0.3$  ( $t=0.41$  s)

The maximum forces of  $F_y$  and  $F_z$  increase as the baffle is lowered (Figs. 13a and 13b) except for the curves of  $D=0.1$  and  $D=0.2$ . When  $D \geq 0.3$ , the higher the baffle, the smaller are the forces acting on the tank. Fig. 18 shows the maximum forces with the baffle in different positions.

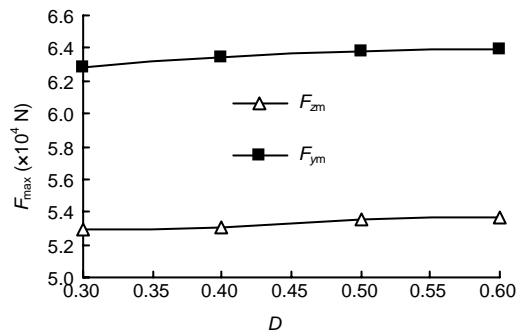


**Fig. 18** The maximum of  $F_y$  and  $F_z$  during turning

One of the important forces affecting transverse stability is the rolling moment. The rolling moment  $M$  in this study is the force acting on a single compartment about an axis through the point of  $R$  and parallel to axis  $x$  in Fig. 1. The rolling moment  $M$  and the maximum of the rolling moment  $M_{max}$  at different time points are shown in Figs. 19 and 20.

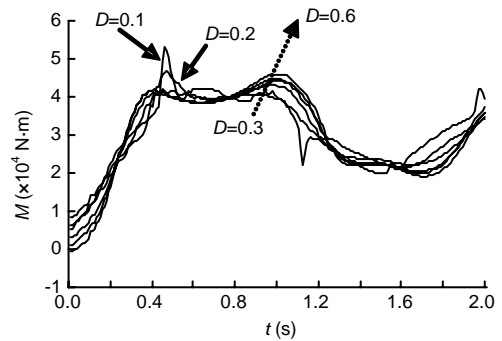


**Fig. 19** The rolling moment during turning

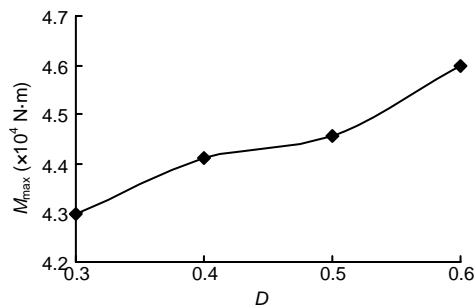


Fig. 20 Maximum rolling moment during turning

Liquid splashing causes the significant crest of the rolling moment at  $D=0.1$  and  $D=0.2$ . When  $D \geq 0.3$ , the crest of the rolling moment increases as the baffle is lowered.

## 5 Conclusion

When the tank truck is braking, at  $A=0.1$ , liquid splashes in the tank and the maximum forces and weight distribution ratio  $G$  are large. When  $A \geq 0.2$ , as the position of the baffle is lowered, the maximum of  $F_x$  first decreases and then increases, reaching a minimum at  $A=0.3$ . The maximums of  $F_y$  and  $G$  increase, the highest position of  $F_x$  becomes higher and the position of  $F_y$  moves backwards.

When the tank is turning, at  $D \leq 0.2$ , liquid splashes in the tank and the maximum forces and  $M$  are large. When  $D \geq 0.3$ , as the position of the baffle is lowered, the maximums of  $F_y$ ,  $F_z$  and  $M$  increase.

## References

- Armenio, V., 1996. On the analysis of sloshing of water in rectangular containers: Numerical study and experiment validation. *Ocean Engineering*, **23**(8):705-737. [doi:10.1016/0029-8018(96)84409-X]
- Bao, G.W., 2002. Approximate calculation of liquid slosh in Dewar. *Chinese Quarterly of Mechanics*, **23**(3):311-314 (in Chinese).
- Chen, Z.W., 2006. Numerical Simulation of Liquid Sloshing in Transportable Pressure Vessel and Research on the Baffles. MS Thesis, School of Material and Chemical Engineering, Zhejiang University, China (in Chinese).
- Cho, J.R., Lee, H.W., 2004. Numerical study on liquid sloshing in baffled tank by nonlinear finite method. *Computer Methods in Applied Mechanics and Engineering*, **193**(23-26):2581-2598. [doi:10.1016/j.cma.2004.01.009]
- Eswaran, M., Saha, U.K., Maity, D., 2009. Effect of baffles on a partially filled cubic tank: numerical simulation and experimental validation. *Computers and Structures*, **87**(3-4):198-205. [doi:10.1016/j.compstruc.2008.10.008]
- Gedikli, A., Erguven, M.E., 2003. Evaluation of sloshing problem by variational boundary element method. *Engineering Analysis with Boundary Elements*, **27**(9):935-943. [doi:10.1016/S0955-7997(03)00046-8]
- Hasheminejad, S.M., Aghabeigi, M., 2009. Liquid sloshing in half-full horizontal elliptical tanks. *Journal of Sound and Vibration*, **324**(1-2):332-349. [doi:10.1016/j.jsv.2009.01.040]
- Kim, Y.S., Yun, C.B., 1997. A spurious free four node displacement based fluid element for fluid structure interaction analysis. *Engineering Structures*, **19**(8):665-678.
- Li, S., Gao, F.Q., Yang, Y.R., Fan, C.G., 2007. Finite element modal analysis and dynamic experimental for liquid sloshing. *Nuclear Power Engineering*, **28**(4):54-57 (in Chinese).
- Liao, Y.X., Wang, H.M., Wang, M.H., 1999. Stress analysis of storing liquid vessel during emergency braking corresponding. *Packaging Engineering*, **20**(3):58-60 (in Chinese).
- Liu, D.M., Lin, P.Z., 2009. Three-dimensional liquid sloshing in a tank with baffles. *Ocean Engineering*, **36**(2):202-212. [doi:10.1016/j.oceaneng.2008.10.004]
- Maleki, A., Ziyaeifar, M., 2008. Sloshing damping in cylindrical liquid storage tanks with baffles. *Journal of Sound and Vibration*, **311**(1-2):372-385. [doi:10.1016/j.jsv.2007.09.031]
- Panigrahy, P.K., Saha, U.K., Maity, D., 2009. Experimental studies on sloshing behavior due to horizontal movement of liquids in baffled tanks. *Ocean Engineering*, **36**(3-4): 213-222. [doi:10.1016/j.oceaneng.2008.11.002]
- Romero, J.A., Hildebrand, R., Martinez, M., Ramirez, O., Fortanell, J.M., 2005. Natural sloshing frequencies of liquid cargo in road tankers. *International Journal of Heavy Vehicle Systems*, **12**(2):121-138. [doi:10.1504/IJHVS.2005.006379]
- Yue, B.Z., Wang, Z.L., Li, J.F., 1996. Liquid sloshing in cylindrical tank with elastic spacer. *Communications in Nonlinear Science & Numerical Simulations*, **1**(2):66-69.